compared with several models. There was qualitative but not quantitative agreement with the random packing model. There was reasonably good agreement with the quasicrystalline model, except for the precise shape of the first peak and two extra oscillations in the calculated density function. A method was devised for calculating radial density functions using the assumptions of the tunnel model. The calculated density functions agreed very well with experimental measurements, but the results are based on parameters which cannot be predicted theoretically at this time. Nevertheless, the tunnel model possesses enough features to warrant further investigation.

ACKNOWLEDGMENTS

The authors would like to acknowledge the Office of Naval Research for their support of this research and the MIT Computation Center for their support of the phases of the work which involved the computer. They are specially indebted to S. L. Strong for his assistance throughout the course of the research.

PHYSICAL REVIEW VOLUME 150, NUMBER 1 7 OCTOBER 1966

Resonant Electron-Capture Measurements of Close He^{++}—He and He^{++}—H Collisions*

WILLIAM C. KEEVER AND EDGAR EVERHART
Physics Department, The University of Connecticut, Storrs, Connecticut
(Received 25 May 1966)

Differential measurements of close single collisions are made for the reaction $He^{++}+He \rightarrow He+He^{++}$ in which the probability P_0 for double electron exchange is found to be an oscillating function of incident energy. Similar measurements for the reaction $He^{++}+He \rightarrow He^{+}+He^{+}$ show that the probability P_1 for exchange of a single electron (plotted versus reciprocal velocity) oscillates at twice the frequency of the P_0 oscillations. Close encounters in the one-electron collision $He^{++}+H \rightarrow He^{+}+He^{+}$ are also studied here, and the probability P_1 of electron exchange plotted versus energy shows an oscillation of low amplitude. The experiments encompass incident He^{++} energies in the range of 2 to 200 keV and scattering angles between 1.2° and 3.0°. The data are discussed using energy-level diagrams of the $HeHe^{++}$ and HeH^{++} systems.

I. INTRODUCTION

EXPERIMENTS studying close encounters in ion-atom collisions have shown resonant electron capture phenomena to occur in a number of symmetrical ion-atom combinations.[1] The present experiment shows that there is a similar phenomenon in He^{++}–He collisions which might be termed resonant *double* electron capture. In the reaction

$$He^{++}+He \rightarrow He+He^{++}, \quad (1)$$

the fast alpha particle picks up both electrons in a single close encounter and the probability for double capture is here found to be a resonant or oscillating function of incident energy.

This phenomenon in the He^{++}–He system was predicted by Lichten[2,3] and by Basu, Mukherjee, and Sil.[4] It is shown here that the predictions[2–4] regarding spacings (versus reciprocal velocity) of the capture-probability peaks are in good qualitative agreement with the data. Lichten[2] made the further remarkable prediction that the *single* electron-capture probability in the competing reaction

$$He^{++}+He \rightarrow He^{+}+He^{+} \quad (2)$$

would oscillate with twice the frequency of the *double* electron-capture probability. This prediction by Lichten is indeed borne out by the present data.

Measurements of the unsymmetrical He^{++}–H combination are also presented. This is, after H^{+}–H, practically the only other one-electron combination which it is feasible to study.[5] This combination is accidentally resonant (with zero energy deficit) according to

$$He^{++}+H(1s) \rightarrow He^{+}(2s \text{ or } 2p)+H^{+} \quad (3)$$

if the incident particle is left in an $n=2$ state after the

* This work was sponsored by the U. S. Army Research Office, Durham, North Carolina.

[1] Experimental work: H^{+}–H: G. J. Lockwood and E. Everhart, Phys. Rev. **125**, 567 (1962); H. F. Helbig and E. Everhart, *ibid.* **140**, A715 (1965); He^{+}–He: G. J. Lockwood, H. F. Helbig, and E. Everhart, *ibid.* **132**, 2078 (1963); D. C. Lorents and W. Aberth, *ibid.* **139**, A1017 (1965). Other experiments and the related theoretical papers are discussed in the above papers.

[2] W. Lichten, Phys. Rev. **131**, 229 (1963).

[3] W. Lichten, Phys. Rev. **139**, A27 (1965).

[4] D. Basu, S. C. Mukherjee, and N. C. Sil, in *Proceedings of the Third International Conference on Physics of Electronic and Atomic Collisions, London, 1963*, edited by M. R. C. McDowell (North-Holland Publishing Company, Amsterdam, 1964), p. 769.

[5] Almost the only other one-electron combinations are Li^{+++}–H and He^{+}–H^{+}, both of which would offer great difficulties for these differential-cross-section measurements.

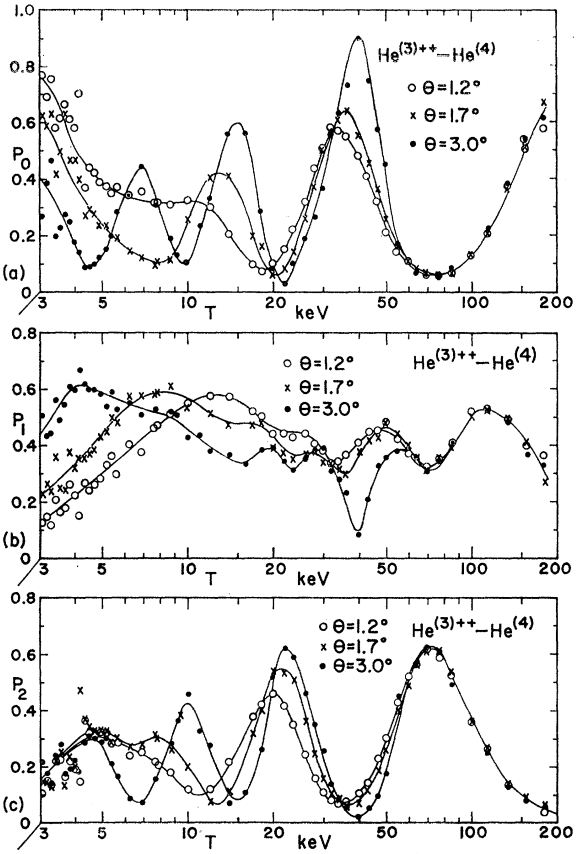

FIG. 1. (a) For the $He^{(3)++}$–$He^{(4)}$ collision, the values of double-electron-capture probability P_0 are plotted versus incident-ion energy T at the laboratory scattering angles θ of 1.2°, 1.7°, and 3.0°. (b) The same as for (a), except that the single-electron-capture probability P_1 is plotted. (c) The same as for (a), except that the probability P_2 of scattering without change of charge is plotted.

collision. Bates and Lynn[6] have discussed the theory of the accidentally resonant case, but they made no numerical calculations directly applicable here.

For the He^{++}–H combination, Fite, Smith, and Stebbings[7] have measured the *total* capture cross section. Some of the theory is the same, and we share their experimental difficulties in working with He^{++} beams and atomic hydrogen targets. However, the present measurements are of a differential character, being concerned only with close encounters, i.e., those rare collisions with small impact parameter.

Other unsymmetrical ion-atom combinations which have been studied experimentally[8,9] and which show interesting structure in close encounters are H^+–He, H^+–Ne, H^+–Ar, and Ne^+–Ar. However, charge exchange in these combinations involves a change in energy, and the present He^{++}–H study is the first such experiment where there may be accidental resonance.

II. THE EXPERIMENT

The apparatus used here is identical to that used in several other experiments in our laboratory,[1] and the procedure is also essentially the same. Particles undergoing a single close encounter with a target atom are selected according to their angle of scattering, and the number in various states of charge after collision are counted individually. Here P_0 is the fraction of the fast particles which are neutral after scattering, P_1 is the fraction which are singly ionized, and P_2 is the fraction which are doubly ionized.

The He^{++} ion beam is formed in an rf ion source with about 1% the abundance of the singly ionized beam from the same source. Ordinarily, a He^{++} beam would have the same charge/mass ratio (and also the same magnitude of current) as the H_2^+ contaminant beam from the source, and these would not be separated in the accelerator's analyzing magnet. For this reason helium of mass three is used in our source, for then the $He^{(3)++}$ beam is alone in its charge/mass ratio and can be separated cleanly from all other ions.

For the He^{++}–H combination, the target chamber is a tungsten furnace containing hydrogen gas over 90% dissociated with the furnace at 2400°K. The construction and operation of this furnace have been described.[1,10]

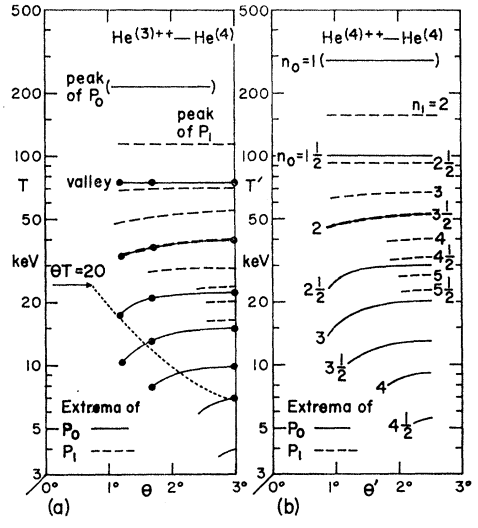

FIG. 2. (a) These data concern the $He^{(3)++}$–$He^{(4)}$ collision. The locations of the maxima (peaks) and minima (valleys) of double-electron-capture P_0 are shown as solid lines on T-versus-θ axes. The maxima and minima of single-electron-capture probability P_1 are shown as dashed lines. (b) A corresponding plot is made for the (unmeasured) $He^{(4)++}$–$He^{(4)}$ collision. Here the successive maxima and minima of P_0, as indicated by the solid lines, are labeled by an index n_0 and those of P_1 as indicated by the dashed lines, are labeled by an index n_1.

[6] D. R. Bates and N. Lynn, Proc. Roy. Soc. (London) **A253**, 141 (1959).

[7] W. L. Fite, A. C. H. Smith, and R. F. Stebbings, Proc. Roy. Soc. (London) **A268**, 527 (1962).

[8] H. F. Helbig and E. Everhart, Phys. Rev. **136**, A674 (1964).

[9] F. P. Ziemba, G. J. Lockwood, G. H. Morgan, and E. Everhart, Phys. Rev. **118**, 1552 (1960).

[10] G. J. Lockwood, H. F. Helbig, and E. Everhart, J. Chem. Phys. **41**, 3820 (1964).

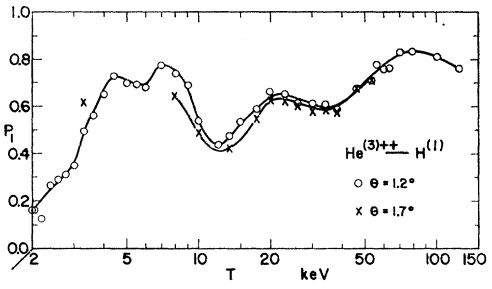

FIG. 3. These data concern the $He^{(3)++}$–$H^{(1)}$ collision. Here the single-electron-capture probability P_1 is plotted versus incident-ion energy T for scattering angles θ of 1.2° and 1.7°.

III. DATA

Figure 1(a) shows data for the $He^{(3)++}$–$He^{(4)}$ case plotting P_0, which is the probability of double electron capture, versus incident ion energy T at the three laboratory angles θ of 1.2°, 1.7°, and 3°. Figure 1(b) shows a similar plot of P_1, which is a measure of the He^+ scattered component, and Fig. 1(c) shows the plot for P_2 which is a measure of the He^{++} scattered component. Of course, $P_0+P_1+P_2=1$ here. Although the peaks and valleys of P_1 in Fig. 1(b) are of uneven height, a plot of the ratio P_1/P_2 would show more regularity in this respect.

Figure 2(a) shows the locations of maxima and minima of P_0 as solid lines and those of P_1 as dashed lines. These are plotted with the incident energy T as ordinate and the laboratory scattering angle θ as abscissa. These contours have the same general form as the corresponding experimental plots[1] for H^+–H and He^+–He. Figure 2(b) shows the equivalent contours for the (unmeasured) $He^{(4)++}$–$He^{(4)}$ case where the axes are T' and θ'. It may be easily shown, for the same distance of closest approach and the same velocity, that

$$T'=\tfrac{4}{3}T, \quad \theta'=\tfrac{3}{4}\theta, \quad \text{and} \quad \theta T=\theta' T'. \qquad (4)$$

The contours on Fig. 2 stop for values of θT or $\theta' T'$ below about 12 deg keV. Although there are data in Fig. 1 at smaller values of θT, the oscillations are apparently no longer present. In Fig. 2(b) the contours for P_0 are labeled by an index n_0 starting with $n_0=1$ at the highest energy peak, $n_0=1\frac{1}{2}$ for the valley below, $n_0=2$ for the next peak, etc. The index n_1 refers to peaks and valleys of P_1 in a similar manner.

The $He^{(3)++}$–$H^{(1)}$ combination is shown in Fig. 3, which plots P_1 versus incident energy at $\theta=1.2°$ and 1.7°. Of course it is not known whether the $He^{(3)+}$ after scattering is in the $(2s)$ or $(2p)$ state indicated by Eq. (3). In Fig. 3 it is not necessary to show P_2, since $P_1+P_2=1$ in this case.

IV. DISCUSSION

A. The He^{++}–He Collision

It is useful to consider sets of data for which the product θT is a constant, for these sets correspond to constant values[11,12] of distance of closest approach R_0. Thus along the dotted line labeled $\theta T=20$ deg keV in Fig. 2(a) the value of R_0 is constant, although incident energy (and hence velocity) vary along this line. One computes the velocity v corresponding to each energy where n_0 contours cross this dotted line. Plotting $n_0-\frac{1}{2}$ versus $1/v$ as in Fig. 4 gives the sequence of points labeled $\theta T=20$ deg keV, and these appear to lie on a straight line. Other values of θT give points on other straight lines as shown. This figure is rather similar to the corresponding plot[12] for He^+–He.

The linear relationship is consistent with the theories.[2–4] Thus $n_0-\frac{1}{2}$ is a measure of the number of oscillations occurring during the collision, and $1/v$ is proportional to the collision time. A similar plot versus $1/v$ is made on Fig. 4 for $n_1-\frac{1}{2}$ values which correspond to the P_1 oscillations, and these lie on a straight line of about twice the slope.

Figure 5 shows certain relevant energy levels for $HeHe^{++}$ and He^+He^+ plotted versus internuclear distance R. The curves labeled $(\sigma_g)^2$ and $(\sigma_u\sigma_g)$ have been calculated with good accuracy by Michels.[13] The curve labeled $(\sigma_u)^2$ presents problems: The adiabatic level, as calculated by Michels, follows the dashed line which bends downward because of an avoided crossing with another level not shown. The adiabatic level, as estimated qualitatively by Lichten (in Fig. 6 of Ref. 3), crosses many other levels (not shown) and finally connects at $R=0$ to the doubly excited state $Be^{++}(2p)^2$. This is an auto-ionization level lying far within the continuum.

According to theory[2–4] and to the example of other data analyses,[12] the slope of the $n_0-\frac{1}{2}$ lines in Fig. 4 can be obtained, approximately, from the area between the *gerade* and *ungerade* energy levels. This area is shaded in Fig. 5. Specifically, twice the area in question,

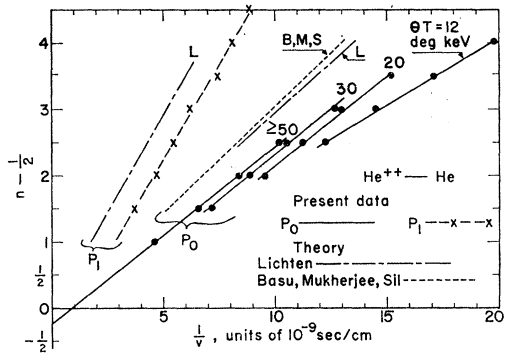

FIG. 4. For the He^{++}–He collision a quantity $n-\frac{1}{2}$ is plotted versus reciprocal velocity $1/v$. Data taken at constant values of θT correspond to collisions where distance of closest approach R_0 is held constant. Values of $n_0-\frac{1}{2}$ for the P_0 oscillations and $n_1-\frac{1}{2}$ for the P_1 oscillations are both shown together with theoretical predictions by Lichten and by Basu, Mukherjee, and Sil.

[11] P. R. Jones, P. Costigan, and G. Van Dyk, Phys. Rev. **129**, 211 (1963).
[12] E. Everhart, Phys. Rev. **132**, 2083 (1963).
[13] H. H. Michels (private communication).

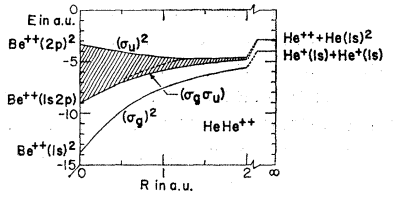

FIG. 5. Electronic energies are given versus interatomic distance R for the $HeHe^{++}$ and $He^{+}He^{+}$ systems. These are derived from the work of Lichten (Refs. 2 and 3) and Michels (Ref. 13).

divided by Planck's constant, gives the corresponding slope[12] (for the case of large θT or small R_0). In this way we have calculated the line marked "L" shown in Fig. 4, so marked because it depends entirely on the identification and estimated values of the $(\sigma_u)^2$ curve as given by Lichten.[2,3] Although Basu, Mukherjee, and Sil[4] do not present an energy-level diagram, they do calculate a quantity which is equivalent to the spacing between the *gerade* and *ungerade* levels and their result corresponds to the line marked "BMS" on Fig. 4. Both the lines, "L" and "BMS" are drawn for the case of small R_0, or large θT, and agree fairly well with the data.

Lichten's analysis, which is qualitative, made the further prediction that oscillations will be found in P_1 also and that these oscillations will be of roughly twice the frequency of the P_0 oscillations.[14] Accordingly, another line marked "L" has been added to Fig. 4 with twice the slope of the first such line. Indeed, the data points for the P_1 oscillations fit well with this prediction by Lichten.

Following the procedures outlined in Ref. 12 and using the average of the $(\sigma_u)^2$ and $(\sigma_u\sigma_g)$ for the electronic energies, we have calculated θT versus R_0 for the He^{++}–He collision, as presented in Table I. This calculation is approximate. More accurate results would be obtainable following the calculation procedure outlined by Marchi and Smith.[15] It is interesting that the oscillations are only seen on Fig. 1 for $\theta T > 12$ deg keV, and this corresponds to $R_0 < 0.48$ atomic units. Unless the collisions are sufficiently violent to cause the internuclear distance to be less than this value, the oscillations are not seen. In this respect the He^{++}–He collision appears to be different from the H^{+}–H and He^{+}–He cases.

TABLE I. Computed values of θT are given for various distances of closest approach R_0 for the He^{++}–He and the He^{++}–H systems. The values labeled "screened" allow for electronic energies, as explained in the text, and those labeled "Rutherford" do not allow for electron screening.

	θT (deg keV)			
	He^{++}–He		He^{++}–H	
R_0 (a.u.)	Screened	Rutherford	Screened	Rutherford
0.1	62.0	62.4	31.0	31.2
0.2	30.1	31.2	15.5	15.6
0.3	20.6	20.8	10.4	10.4
0.4	14.7	15.6	7.77	7.80
0.5	11.3	12.5	6.23	6.24
0.6	8.99	10.4	5.13	5.20
0.8	5.95	7.80	3.76	3.90
1.0	4.05	6.24	2.91	3.12
1.2	2.86	5.20	2.32	2.60
1.4	2.01	4.46	1.79	2.23

B. The He^{++}–H Collision

The data curves of Fig. 3 show a weak oscillation. It is informative to assign integral and half-integral values to an index n_1 and plot this versus reciprocal velocity, as in Fig. 6, where the data for $\theta = 1.2°$ are seen to lie fairly well on a straight line. Although the data are not extensive enough to draw this line for constant θT, the slope of this line is still an approximate measure of the oscillation frequency. This slope, multiplied by Planck's constant, is $\langle Ea \rangle = 80$ eV Å, or 5.5 in atomic units (a.u.) of energy×distance.

This $\langle Ea \rangle$ value gives a clue as to the transition responsible for the oscillation, which may be seen by studying the energy-level diagram. Bates and Carson[16] have calculated the HeH^{++} states, and these electronic energies are shown plotted versus R in Fig. 7. If, indeed, the accidentally resonant reaction of Eq. (3) were responsible for the resonance, then the area between the $2p\sigma$ and the average of the $2p\pi$ and $2s\sigma$ states, integrated over a range in R out to some value λ', should equal half the above $\langle Ea \rangle$ value, or 2.75 in atomic units. This reasoning is analogous to that of the theory of the symmetric-resonant case, which such a relationship holds rather closely. However, the states in question are too close together; in order to pick up sufficient area it is necessary to integrate out to $\lambda' \approx 13$ a.u., which is an impossibly large distance for the electron exchange to occur. The conclusion is that the accidentally resonant reaction is not responsible for the oscillations seen.

On the other hand, we can tentatively assign the oscillation to the $2p\sigma$–$1s\sigma$ transition which is widely

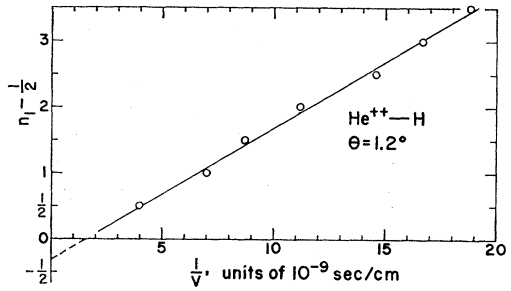

FIG. 6. For the He^{++}–H collision, a quantity $n_1 - \frac{1}{2}$ is plotted versus reciprocal velocity $1/v$ for data taken at $\theta = 1.2°$.

[14] This prediction concerning P_1 oscillations appears in Fig. 6 and in Eqs. (22) and (23) of Ref. 2. There is a misprint in Lichten's Eq. (23) which should read $P_1 = \frac{1}{2}\sin^2\phi_1$ in his notation. See also Sec. II B of Ref. 3.

[15] R. P. Marchi and F. T. Smith, Phys. Rev. **139**, A1025 (1965).

[16] D. R. Bates and T. R. Carson, Proc. Roy. Soc. (London) A234, 207 (1956).

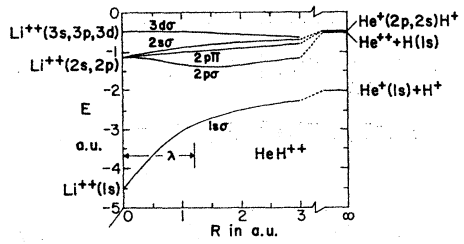

FIG. 7. Electronic energies are given versus interatomic distance R for the $He^{++}H$ and $He^{+}H^{+}$ systems. These are plotted from the calculations of Bates and Carson (Ref. 15).

spaced. Reasoning by analogy with the approximate treatment by Lichten[2,3] (as applied to the nonresonant case), we conclude that the area between these curves between $R=0$ and $R=\lambda$ should be a measure of the oscillation frequency. We find that the required area of 2.75 in atomic units can be found by integrating the area between the $2p\sigma$–$1s\sigma$ lines out to $\lambda=1.2$ a.u. and this dimension is shown on the diagram. This is a reasonable limit to the interaction distance and suggests that the reaction responsible for the oscillation is thus identified.

For reference, the very approximate relationship between θT and R_0 for the He^{++}–H case has also been included in Table I. The electronic energies used are those of the $2p\sigma$ state averaged with values midway between the $2p\pi$ and $2s\sigma$ states.

ACKNOWLEDGMENTS

We have found discussions with Professor W. Lichten of Yale University to be most helpful. The kindness of Dr. H. H. Michels of United Aircraft Research Laboratories in calculating certain energy levels of $HeHe^{++}$, and allowing us to use these in our level diagrams prior to his publication, is much appreciated.

PHYSICAL REVIEW VOLUME 150, NUMBER 1 7 OCTOBER 1966

Proof of a Conjecture by Moszkowski for the Variances of Spectral-Line Distributions

JAY M. PASACHOFF*
Harvard College Observatory, Cambridge, Massachusetts
(Received 31 March 1966)

Moszkowski has suggested that the variances of distributions of spectral lines for transitions of the form $l^n \rightarrow l^{n-1}l'$ can be given in terms of the variance for the two-electron $l^2 \rightarrow ll'$ transition by

$$\sigma^2(l^n \rightarrow l^{n-1}l') = \frac{(n-1)(N_0-n)}{(N_0-2)}\sigma^2(l^2 \rightarrow ll'),$$

assuming that the l' electron in the final state does not interact with the remaining l^{n-1} configuration. Probability matrices are used to prove this conjecture.

I. INTRODUCTION

THE means and variances of interaction energies of configurations of the form l^n and of line distributions for transitions from such configurations to those of the form $l^{n-1}l'$, neglecting the interaction of the l' electrons with the l electrons, has been studied by Moszkowski.[1] He also neglected the splitting of terms by the spin-orbit interaction.

It is known[2] that the n-electron mean interaction energy is related to the two-electron mean interaction energy by

$$\langle E(l^n)\rangle = \binom{n}{2}\langle E(l^2)\rangle, \quad (1)$$

and it can easily be shown that

$$\langle E(l^n \rightarrow l^{n-1}l')\rangle = (n-1)\langle E(l^2 \rightarrow ll')\rangle. \quad (2)$$

Moszkowski carried out explicit calculations for a number of configurations, using tables that can be found in Bacher and Goudsmit,[3] Menzel and Goldberg,[4] and Racah.[5] He was led by this numerical evidence to conjecture that the variances of the energy level and line distributions for configurations of equivalent particles are

$$\sigma^2(l^n) = \frac{\binom{n}{2}\binom{N_0-n}{2}}{\binom{N_0-2}{2}}\sigma^2(l^2), \quad (3)$$

* National Science Foundation Cooperative Graduate Fellow.

[1] S. A. Moszkowski, Progr. Theoret. Phys. (Kyoto) **28**, 1 (1962).

[2] J. C. Slater, *Quantum Theory of Atomic Structure* (McGraw-Hill Book Company, Inc., New York, 1960), Vol. I.

[3] R. F. Bacher and S. Goudsmit, Phys. Rev. **46**, 948 (1934).

[4] D. H. Menzel and L. Goldberg, Astrophys. J. **84**, 1 (1936).

[5] G. Racah, Phys. Rev. **63**, 367 (1943).